Supplementary Information (SI) for Dalton Transactions.
This journal is © The Royal Society of Chemistry 2025

Unveiling the Structural and Electrochemical Effects of Al_2O_3 Incorporation within LiPON Electrolyte Thin Films by Atomic Layer Deposition

Ilyass GHANDARI [a], Nicolas GAUTHIER [a], Névine ROCHAT [a], Sylvain POULET [a], Lara CASIEZ [a], Manon LETICHE [a], Violaine SALVADOR [a], Hélène COUDERT-ALTEIRAC [a], Nicolas VAXELAIRE [a], Mikhael BECHELANY [a] and Messaoud BEDJAOUI [a]

[a]Univ. Grenoble Alpes, CEA LETI, 38054 Grenoble, France

[b]Institut Européen des Membranes-IEM, Univ Montpellier, CNRS, ENSCM, 34095 Montpellier, France

Corresponding Authors

Ghandari Ilyass - Université Grenoble Alpes, CEA LETI, 38054, Grenoble, France

https://orcid.org/0009-0001-9156-9109

Email: ilyass.ghandari@cea.fr

Bedjaoui Messaoud - Université Grenoble Alpes, CEA LETI, 38054, Grenoble, France

Email: messaoud.bedjaoui@cea.fr

Contents table

Supporting Information

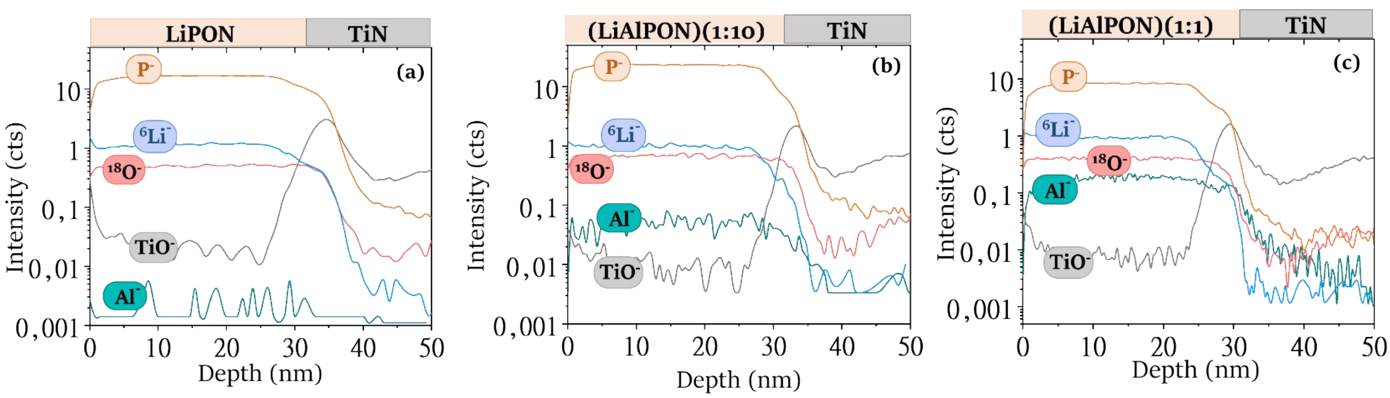

Figure S1. Survey depth profiles as measured with ToF-SIMS of **(a)** LiPON, **(b)** $LiAlPON_{(10:1)}$ and **(c)** $LiAlPON_{(1:1)}$ doped film

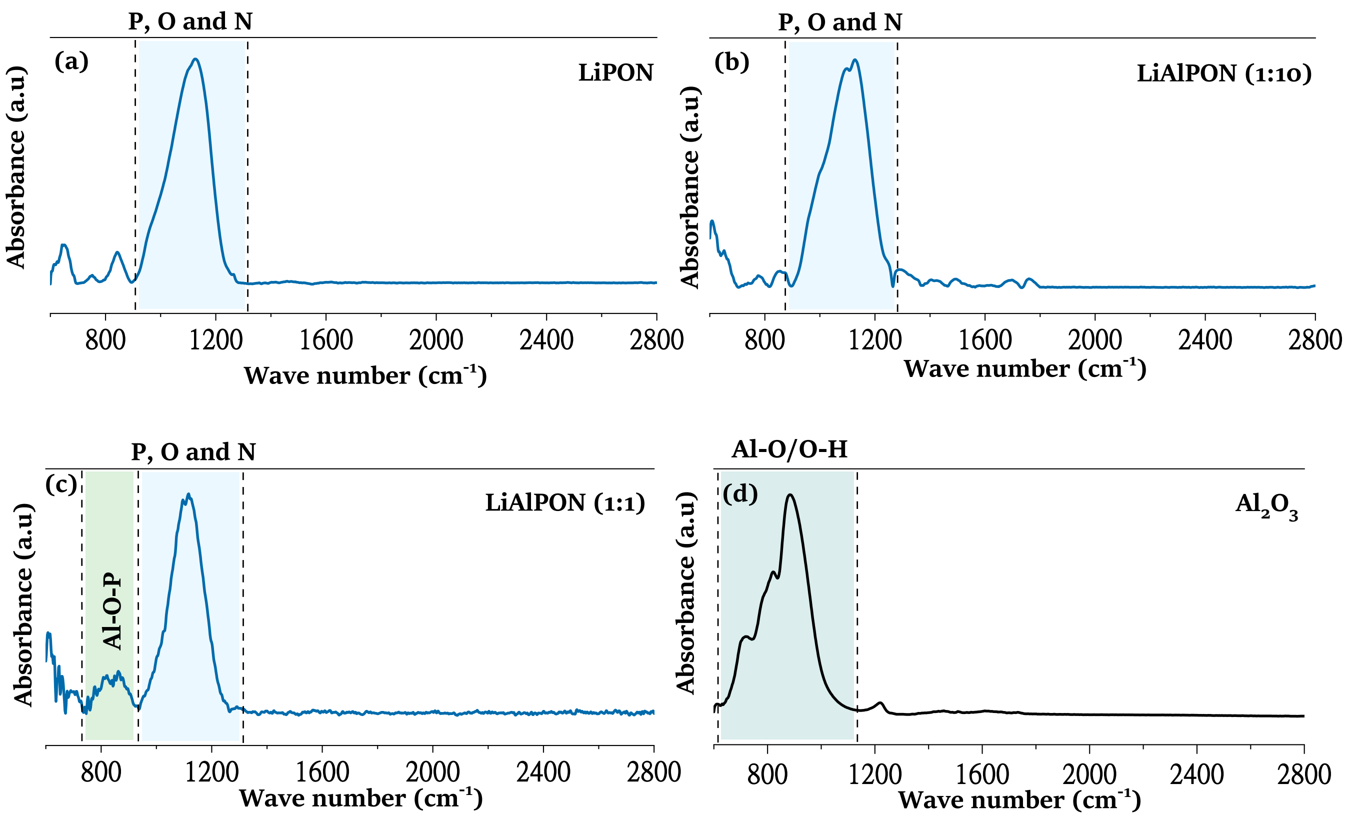

Figure S2. Full FTIR spectra of LiPON films as a function of Al_2O_3 incorporation: (a) LiPON, (b) LiAlPON(10:1) (c) LiAlPON(1:1) (d) Al_2O_3.

The 30 nm thin films were deposited on Si substrates and recorded in the 600–2800 cm^{-1} range. For LiPON-based films, the main FTIR peaks appear between 850 and 1250 cm^{-1}, corresponding to phosphate units. In contrast, the spectrum of the pure Al_2O_3 film shows a major peak shifted to 700–1000 cm^{-1}, primarily arising from Al–O and Al–O–Al bindings. The evolution of these spectral features highlights the structural effect of Al_2O_3 incorporation. For clarity, peak deconvolution was performed using OriginLab with Gaussian fitting [1].

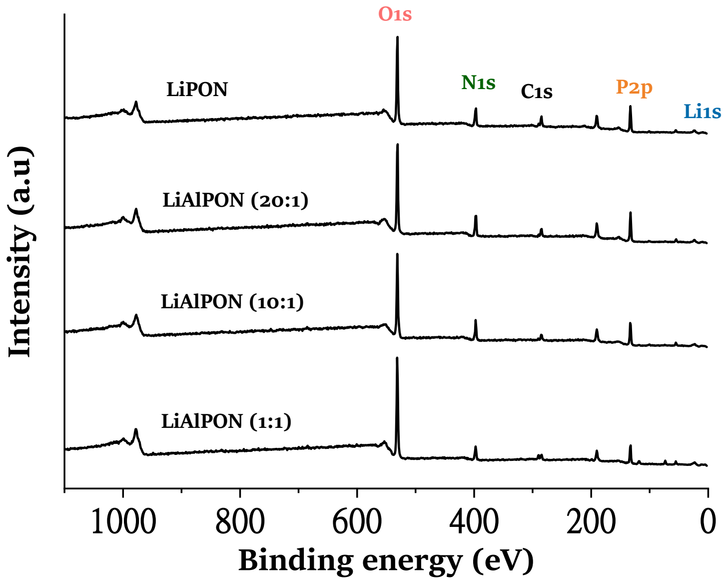

Figure S3. XPS survey spectra of pristine and Al-doped LiPON thin films. The films were deposited on SiO_2 substrates with a thickness of 30 nm. Despite the relatively low energy resolution of the survey spectra, all elements characteristic of LiPON-based films (Li 1s, O 1s, P 2p, N 1s, and C 1s) were clearly detected under different doping conditions and high-resolution scans are used to identify specific functional groups in the article manuscript.

Table S1. Summary of the binding energies and atomic concentrations (at. %) of the different chemical environments identified from the XPS spectra.

Sample Identifier		LiPON		LiAlPON (20 : 1)		LiAlPON (10 : 1)		LiAlPON (1 : 1)	
	Environment	Position	%	Position	%	Position	%	Position	%
O 1s	Li+...O-P	531.3	22.8	531.1	26.4	531.2	26,8	531.3	24.1
O 1s	P-O-P	532.4	3.5	532.4	2.6	532.4	3,2	532.4	3.6
O 1s	P=O	530.9	8.0	530.7	5.5	530.7	2,2	530.8	11.7
O 1s	Li_2O	--	--	--	--	528.6	2,6	528.5	1.1
N 1s	N divalent	397.1	8.9	397.0	9.6	397.1	9,8	397.1	5.0
N 1s	N trivalent	398.8	4.1	398.7	3.3	398.8	2,2	398.9	2.7
C 1s	C-C / C-H	284.9	8.8	284.8	6.1	284.9	5.3	285.0	3,9
C 1s	C-O	286.2	0.7	286.0	0.8	286.1	0.8	286.1	0,4
C 1s	C=O	287.0	0.6	287.0	0.6	287.0	0.4	287.0	0,4
C1s	CO_3^{2-}	289.9	2.0	289.8	1.9	290.0	1.7	289.9	3,5
Li 1s	LiPON / Li_2O	55.3	27.1	55.2	28.9	55.3	31.3	55.3	24,0
P 2p	P2p $_{3/2}$	132.7	8.1	132.6	8.3	132.7	7.7	132.7	5,0
P 2p	P2p $_{1/2}$	133.6	4.0	133.5	4.2	133.6	3.8	133.6	2,5
Al 2p	Al-O	--	--	73.6	0.3	73.4	0.6	73.4	2,6

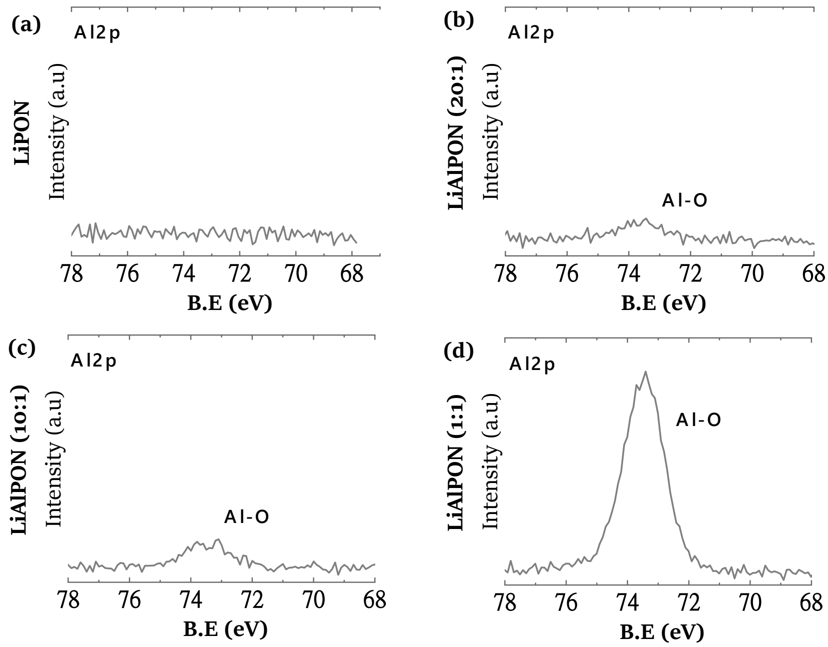

Figure S4. High-resolution Al2p spectra for (a) LiPON, (b) LiAlPON(20:1) (c) LiAlPON(10:1) (d) LiAlPON(1:1).

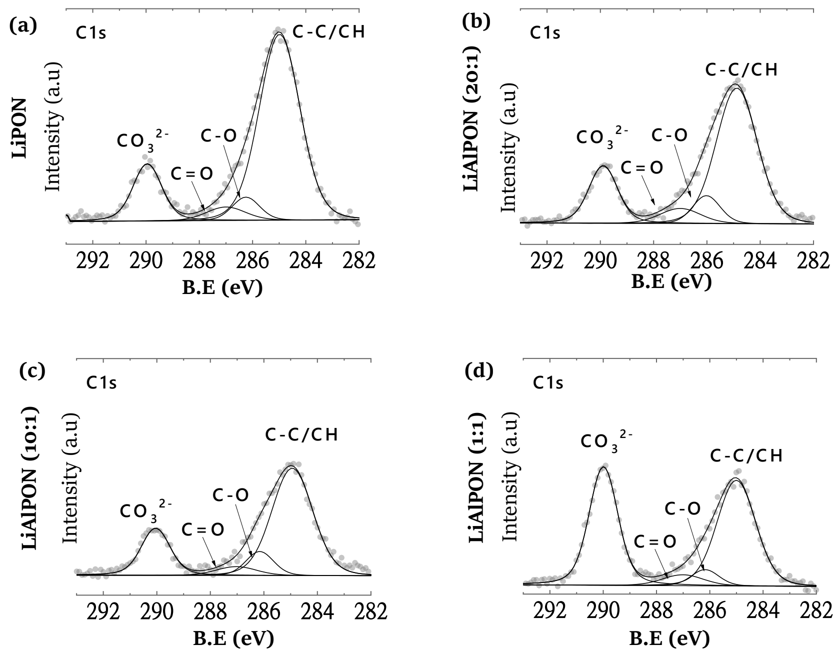

Figure S5. High-resolution C 1s spectra for (a) LiPON, (b) LiAlPON(20:1) (c) LiAlPON(10:1) (d) LiAlPON(1:1). All films exhibit the C–C/C–H hydrocarbon peak at 285 eV. For clarity, a key is provided for each contribution, including C–O, C=O, and CO_3^{2-} groups, observed at 286, 287.5, and 290 eV, respectively [2], [3].

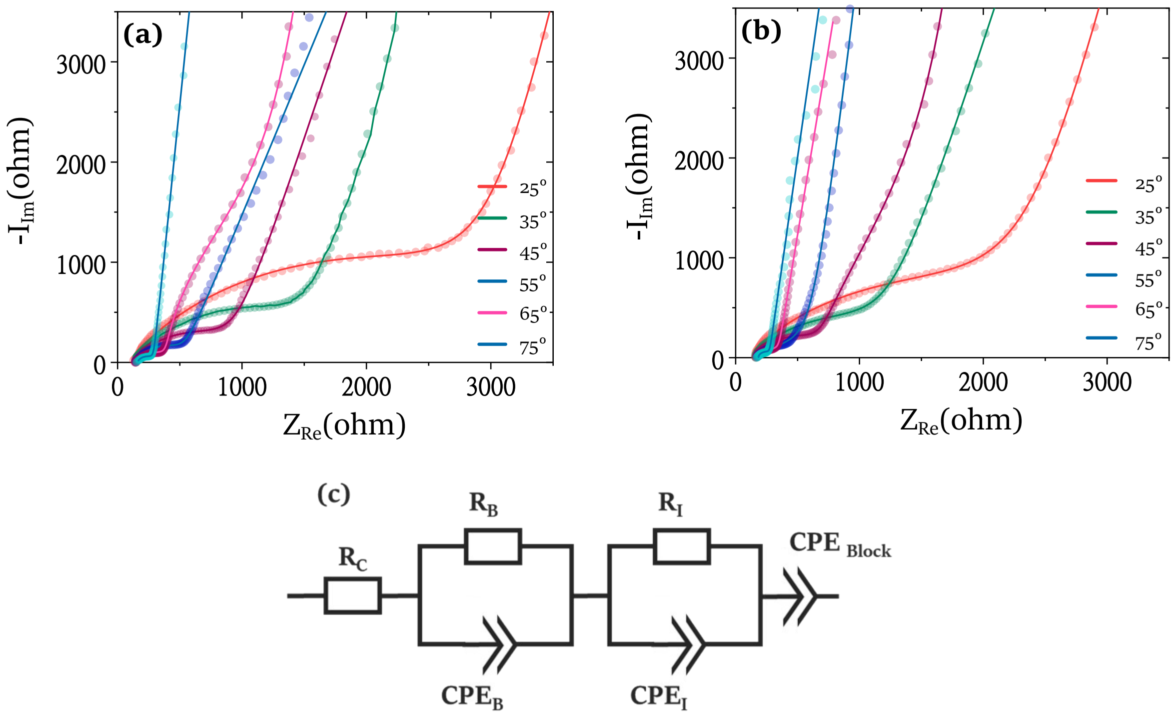

Ionic conductivity was extracted by fitting an equivalent circuit model to the impedance spectroscopy response. The equivalent circuit includes a single contact ohmic resistance, R_c, which corresponds to the high-frequency limiting resistance of the electrode [4]. Ionic conduction processes are modelled using two parallel resistor/constant phase element (CPE) pairs. The first pair, R_B and CPE_B, corresponds to the bulk of the LiPON electrolyte, while the second pair, R_I and CPE_I, represents the resistive layer between Lipon and deposited Pt electrodes. Finally, a single CPE_{dl}, accounts for the formation of the electrochemical double layer at low frequency [5], [6].

Figure S6. Nyquist plots for progressive temperatures ranging from 25 °C to 75 °C for **(a)** LiPON and **(b)** LiAlPON $_{(10:1)}$ **(c)** Equivalent circuit for Nyquist spectra fitting

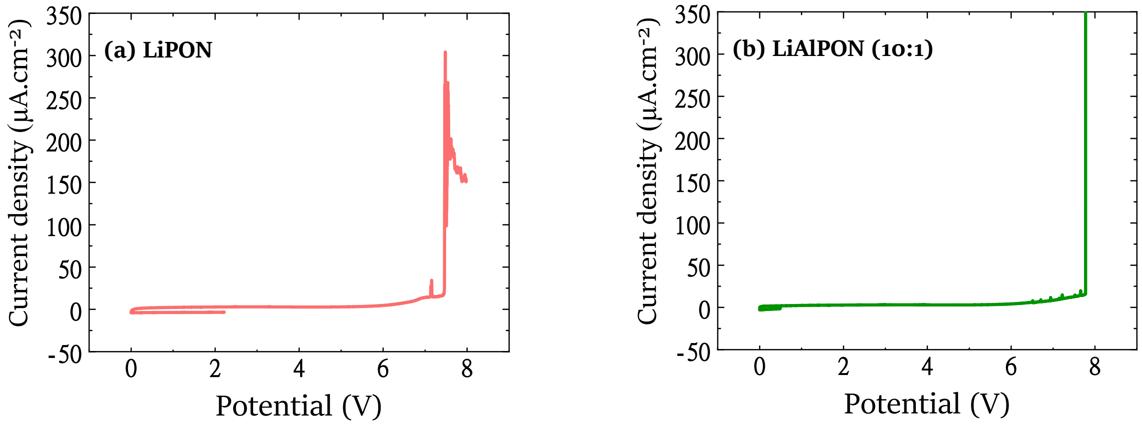

Figure S7. Cyclic voltammograms of **(a)** LiPON and **(b)** $LiAlPON_{(10:1)}$ doped thin films in the voltage range of 0 - 8 V at the scan rate of 100 $mV.s^{-1}$

References

[1] H. T. Kim, T. Mun, C. Park, S. W. Jin, and H. Y. Park, 'Characteristics of lithium phosphorous oxynitride thin films deposited by metal-organic chemical vapor deposition technique', *Journal of Power Sources*, vol. 244, pp. 641–645, Dec. 2013, doi: 10.1016/j.jpowsour.2012.12.109.

[2] M. Nisula, Y. Shindo, H. Koga, and M. Karppinen, 'Atomic Layer Deposition of Lithium Phosphorus Oxynitride', *Chem. Mater.*, vol. 27, no. 20, pp. 6987–6993, Oct. 2015, doi: 10.1021/acs.chemmater.5b02199.

[3] V. Sallaz *et al.*, 'Dual Storage Mechanism in Nanoscale Solid-State Lithium-Ion Supercapacitors', *ACS Electrochem.*, p. acselectrochem.4c00022, Oct. 2024, doi: 10.1021/acselectrochem.4c00022.

[4] T. Tsuruoka, S. Mallik, T. Tsujita, Y. Inatomi, and K. Terabe, 'Effects of Plasma Reactants on Atomic Layer Deposition of Lithium Phosphate and Lithium Phosphorus Oxynitride Electrolyte Films', *Chem. Mater.*, vol. 36, no. 12, pp. 6193–6204, Jun. 2024, doi: 10.1021/acs.chemmater.4c00960.

[5] B. Put, P. M. Vereecken, J. Meersschaut, A. Sepúlveda, and A. Stesmans, 'Electrical Characterization of Ultrathin RF-Sputtered LiPON Layers for Nanoscale Batteries', *ACS Appl. Mater. Interfaces*, vol. 8, no. 11, pp. 7060–7069, Mar. 2016, doi: 10.1021/acsami.5b12500.

[6] T. Tsuruoka, J. Su, and K. Terabe, 'A Voltage-Controlled Oscillator Using Variable Capacitors with a Thin Dielectric Electrolyte Film', *ACS Appl. Electron. Mater.*, vol. 2, no. 9, pp. 2788–2797, Sep. 2020, doi: 10.1021/acsaelm.0c00481.